Desalination and Water Treatment
www.deswater.com

doi:10.5004/dwt.2017.21605

94 (2017) 89–99
October

Effects of polyacrylamide addition and dosage on the effectiveness of sludge-recycling enhanced flocculation

Wei Wei[a,b,*], Jia Zhu[b], Chaosheng Zhang[a], Hongwei Rong[a], Yongfeng Cao[a]

[a]*School of Civil Engineering, Guangzhou University, Guangzhou, China, Tel./Fax: +86-13266518787, email: weiweihit@hotmail.com (W. Wei), gdzcs@126.com (C. Zhang), hwrong@gzhu.edu.cn (H. Rong), 398213541@qq.com (Y. Cao)*
[b]*Department of Building and Environmental Engineering, Shenzhen Polytechnic, Shenzhen, China, email: 7566874@qq.com*

Received 11 May 2017; Accepted 6 November 2017

ABSTRACT

The dosage effect of polyacrylamide (PAM) with long-chain molecule conformation on the effectiveness of Sludge-recycling enhanced flocculation (SEF)at three typical charge states of colloid aggregation was investigated in kaolin (System I) and humic-kaolin (System II) water treatment. The three typical charge states of colloid aggregation were evaluated by the residual turbidity and zeta potential results from traditional flocculation (TF) test with various coagulant dosage. A floc imaging system was employed to investigate the floc characteristics. The experimental results show that the increase in PAM dosage cannot change the effectiveness of SEF for System I in any charge states, compared to TF. However, for System II, SEF was enabled at the PAM dosage of 0.10 mg/L in the state of electrostatic patch (EP) and at 0.20 mg/L in the state of near charge neutrality (NCN). Although the recovery ability was improved and breakability was decreased by the PAM addition, the recovery factor in SEF was lower and breakage factor was higher than that in TF in most cases. With proper PAM dosage, the SEF floc morphology became superior to TF for floc settlement, with less amount of small floc (<50 μm)which may be the direct reason for the effective performance of SEF. Moreover, the results also showed that, when the sweep flocculation (SF) dominates the coagulation mechanism, the addition of PAM was not relevant.

Keywords: Polymer; Sludge-recycling; Electrostatic patch; Charge neutrality; Sweep flocculation

1. Introduction

In coagulation-flocculation based water and wastewater treatment processes, coagulant aids (CAs) are mainly used to enhance the performance efficiency of the primary coagulant and to reduce the process costs [1]. The use of CAs helps to form stronger flocs that resist being broken by particle collision and hydraulic shear force, enhance floc compaction resulting in faster settlement, reduce the optimum primary coagulant dosage and reduce the produced sludge volume. Some of the widely used CAs are synthetic polymer electrolytes such as polyacrylamide (PAM) which are long-chain molecules [2–4]. Adsorption and the bridging of colloidal particles are the main CAs mechanism of PAM in coagulation-flocculation processes [5,6].

*Corresponding author.

Sludge-recycling enhanced flocculation (SEF), earlier known as chemical sludge return [7–9], is a kind of high efficiency water treatment technology that promotes coagulation by controlling sludge return to the specified position such as raw water, rapid mixing stage or slow mixing stage [10–12]. It is generally considered to be a stable, low cost and far superior decontamination method compared to traditional flocculation (TF). However, before the documentary records on the application of CAs in SEF were published, the effectiveness of SEF was debatable.

In our previous paper, the process "re-flocculation after broken" (RAB) was demonstrated to be an effective method to test floc characteristics which are related to the effectiveness of SEF. Our research indicated that, without addition of CAs, the treatment efficiency of SEF was superior to that of TF, and the flocs formed by kaolin and polyaluminum chloride (PACl) under the same working conditions were completely reversible after breakage when low coagulant dosage was used (charge neutrality was the main mechanism). On the contrary, the reinforcement in SEF as well as the reversibility of broken flocs in TF cannot be observed, when restabilization and sweep flocculation occur [13].

In recent publications on natural water or industrial wastewater as raw water, most of the studies considered that SEF showed enhancement of flocculation with the addition of polymer [14–17]. However, some studies still found the optimization of residual turbidity and chemical oxygen demand (COD) without addition of polymer [18,19]. The controversy regarding the use of CA in SEF remains. Considering the wide applications of polyacrylamide (PAM) as CA and its monomer toxicity resulting in usage limitation in various countries [20–22], the necessities of employing PAM aids in SEF must be investigated in detail.

Although many studies have focused on the SEF with CA addition, some significant performances involving internal mechanisms, especially the floc growth, morphology and distribution of matured floc have received insufficient attention. In this paper, two raw water systems treated with kaolin or kaolin and humic acid were used, and image analysis was employed to obtain the information about characteristics of floc formed at three typical charge states (electrostatic patch, near charge neutrality and sweep flocculation). The overall purpose of this study was to investigate the effect of PAM dosage on the strengthening ability of SEF. For comparison purposes, the re-flocculation by TF was also conducted.

2. Materials and methods

2.1. Colloidal system

Preparation of kaolin stock suspension: 100 g kaolin clay was dispersed in 1 L deionized water, and stirred rapidly with a stirring paddle for 2 h. Then, the pH value was adjusted to 8.5 with 0.5 mol NaOH, and after allowing the suspension to stand overnight, the upper layer of the suspension was collected and stored for later use. The particle size distribution of the suspension was measured by a laser particle size analyzer (S3500, Microtrac, USA) ranged from 1 and 20 μm.

Preparation of humic acid stock solution: 15 g sodium humate was dissolved in 1 L deionized water, and the pH value was adjusted to 8.5 with 0.5 mol NaOH under rapid stirring. The solution was stirred further for 1 h. After that, centrifugal separation was conducted and the upper layer of the solution was collected in a brown reagent bottle for later use. A 1 ml stock solution was diluted to 3 L by deionized water, and the value of UV_{254} tested by a UV-visible spectrophotometer was 0.052.

For System I, 50 ml kaolin stock suspension was diluted in 75 L tap water. The alkalinity was adjusted to 120 mg/L (as $CaCO_3$) by 0.5 mol/L $NaHCO_3$ and the pH was adjusted to around 7.9 by 0.5 molar NaOH or 2 mol HCl. For System II, 25 ml of the humic acid stock solution was added into System I. System II was put aside overnight to reach adsorption equilibrium. The two colloidal systems had a turbidity of 40–43 NTU determined by a turbidity meter (Hach, 2100Q, USA). The temperature of the water was 23.8~27.9°C.

2.2. Coagulant and polymers

Commercially available polyaluminum chloride (PACl) with 30% Al_2O_3 content and 40–90% basicity was used to prepare the coagulant solution having 87.43 mg/L of Al in deionized water. The PACl species which is generally divided into three categories: monomeric species (Al_a), medium polymer species (Al_b), and colloidal or solid species (Al_c) [23], was analyzed by Al-Ferron complexation timed spectrophotometry method. The results showed that PACl contained 15.71% of Al_a, 63.43% of Al_b and 20.86% of Al_c.

Anionic polyacrylamide (PAM) with a high molecular weight of 18 million Da (obtained from SNF Floerger) was selected as the coagulant aid. It was diluted to a 0.1% solution and used within 24 h.

2.3. Apparatus and procedure

Experiments were performed using a floc imaging system which was the same as that used by Wei and Li [13]. The raw water was poured into the reactor to the calibration set in advance. The program parameters of blender (for TF: the system was mixed rapidly for 120 s at 300 rpm followed by a 15-min flocculation phase at 70 rpm) and the image capture parameters (one photograph min^{-1} for slow stirring) were set up. After starting the mixing, coagulant and coagulant aids were added according to the scheduled test plan. Finally, the water samples were collected from 3 cm below the liquid surface for a residual turbidity measurement by a portable turbidimeter (Hach, 2100Q, USA) after a 10-min settlement period with no agitation. Each sample was detected 6 times on average. The SEF operating parameters were the same as those of TF, except that the sludge from floc settlement was returned to the raw colloidal system, as shown in Fig. 1.

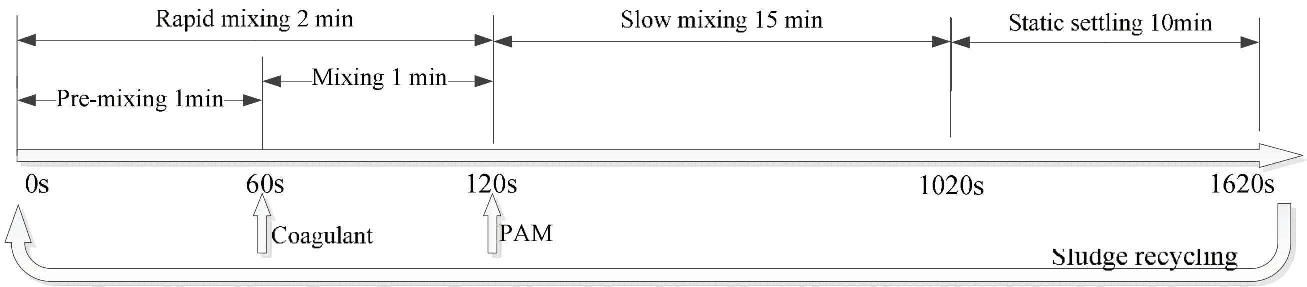

Fig. 1. Schematic diagram of SEF.

The sludge required for enhancement of flocculation was obtained by TF from the controlled trials after discarding the supernatant. Due to the difficulty in controlling the sludge dosage, one-time dosing of sludge produced by a single parallel testis defined as "single-dosage" in order to avoid large errors between the control trials, and similarly, sludge dosing by two parallel tests is defined as twice-dosage. In this study, the sludge addition was all single-dosage.

Coagulant dosages for System I were: 0.91, 1.46, 1.82, 2.73, 3.64, 5.46, 7.29, 10.93, 14.57, 18.21, 27.32, and 36.43 mg/L, and for System II, they were: 3.64, 5.46, 7.29, 9.11, 10.93, 14.57, 18.21, 27.32, and 36.43 mg/L. These coagulant dosages were added at 60 s during the rapid mixing stage. Zeta potential of particulate matter in raw water and 50 s after dosing of coagulant was measured using Zeta potential detector (Brookhaven, 90 Plus Zeta, USA). Each sample was detected 10 times, and then the average was taken after removing the maximum and minimum values. After addition of coagulant, PAM dosages of 0.00 mg/L, 0.05 mg/L, 0.10 mg/L, 0.20 mg/L, and 0.30 mg/L were added at 120 s at the start of the slow mixing.

2.4. Image analysis and data processing

All grayscale pictures collected from the floc imaging system with a size of 1393 × 1040 pixels were processed by a professional image processing software (Image pro-plus 7.0, Media Cybernetics, USA). Each photo was loaded in the software program for background subtraction and binarization processing. The following floc morphological parameters were measured: floc particle count, floc diameter (through the center of mass, average measured values of the secant per 2 rotation degrees), floc perimeter and area. The average of all the floc values in each picture was expressed as corresponding moment of the floc morphological parameters. The floc distribution was obtained from the data processing software by OriginLab 9.0 (OriginLab Corporation, Northampton, MA, USA).

An operational process involving a 60-s rapid breakage stage at 300 rpm followed by a 15-min recovery phase at 70 rpm and a 10-min settlement with no mixing was performed to test the ability of flocs to resist rupture and re-flocculation of broken flocs. The floc breakage factor, as defined by Eq. (1), has been used frequently to characterize flocs [24–26], and the floc recovery factor is defined by Eq. (2),

$$B_f = \frac{d_a - d_b}{d_a} \tag{1}$$

$$Rg_f = \frac{d_c}{d_a} \tag{2}$$

where the terms, d_a, d_b and d_c are the steady-state floc size before breakage, after breakage and after regrowth period, respectively.

The perimeter-based fractal dimension D_{pf} was used to represent the regularity of floc morphology, ranging from 1 (regular, spherical) to 2 (irregular, serrated or linear, non-spherical). The increasing D_{pf} can be explained as follows: when the projected area of fractal floc increases, its perimeter grows more rapidly than Euclidean objects [27–29]. The floc perimeter-area power law relationship was applied to assess the fractal dimension of single floc which is defined by Eq. (3).

$$A \propto P^{2/D_{pf}} \tag{3}$$

where A and P are the projected floc area and perimeter of flocs, respectively.

3. Results and discussion

3.1. Definition of the electrical charge condition

In the electrostatic patch (EP) mechanism, the flocculation occurs in the state of incomplete charge neutrality, in which the electrical property of colloidal surface charge is unchanged, and adequate quantities of hetero-charges should be supplemented to achieve the isoelectric point [30,31]. The near charge neutrality (NCN) means that the surface charge of colloid is very close to electric neutrality. Also, sweep flocculation (SF) signifies charge reversal and excess deposition on the colloidal surface.

The three typical charge states were determined by the residual turbidity and zeta potential after a series of TF tests with different coagulant dosages and without addition of CA. The zeta potential of raw water was –26.67 and –30.80 mV for System I and System II, respectively. From the results shown in Table 1, the coagulant dosages of 1.46 mg/L and 3.64 mg/L were considered to be the EP mechanism for System I and System II, respectively, the dosages of 2.73 mg/L and 7.29 mg/L were marked as NCN and the dosage of 36.43 mg/L was considered as sweep flocculation for both colloidal systems.

3.2. Residual turbidity

At different PAM dosages, the residual turbidity of SEF and TF, and their RAB were measured, and are shown in Fig. 2.

With regard to System I (Fig. 2a), when the reaction was in the state of EP, the increase in PAM dosage brought about higher residual turbidity. Thus, in this state, adding high molecular weight polymer material produced certain colloidal protection, but did not affect the reinforcement impact on TF by SEF, and did not have an impact on the reinforcement of RAB for these two flocculation types. When the reaction was in the state of NCN, the increase in PAM dosage gradually reduced the residual turbidity, and promoted the colloidal particle removal. In this state, the turbidity removal effect of SEF was superior to that of TF, showed the reinforcement effect, and the residual turbidity of their RAB also significantly decreased. However, when the reaction was in the state of SF, the increase in PAM dosage did not obviously improve the effluent quality, which suggests that under this condition, the SEF did not have a reinforcement effect on TF.

The above phenomenon indicated that for System I, the addition of PAM did not change the effect of SEF on TF in the different charge states (whether it performs a strengthening removal of the turbidity or not).

Table 1
Zeta potential and residual turbidity at various coagulant dosages

Coagulant dosage (mg/L)	System I				System II			
	Zeta potential (mV)	Standard deviation	Residual turbidity (NTU)	Standard deviation	Zeta potential (mV)	Standard deviation	Residual turbidity (NTU)	Standard deviation
0.91	–14.35	0.66	15.60	0.28	No data	No data	No data	No data
1.46	–12.64	0.87	6.34	0.33	No data	No data	No data	No data
1.82	–7.61	0.27	4.57	0.29	–23.95	0.40	31.06	0.23
2.73	–2.11	0.49	2.22	0.16	No data	No data	No data	No data
3.64	0.97	2.13	2.17	0.19	–12.45	0.75	9.46	0.25
5.46	3.81	1.33	2.42	0.25	–6.75	0.47	7.38	0.07
7.29	7.83	1.40	1.76	0.12	–1.95	2.18	5.34	0.13
9.11	No data	No data	No data	No data	2.94	1.38	2.20	0.13
10.93	10.57	3.27	2.31	0.27	5.41	1.39	1.46	0.11
14.57	12.69	1.62	2.49	0.33	8.49	1.56	4.83	0.08
18.21	16.15	0.91	2.63	0.19	11.39	0.94	4.99	0.03
27.32	20.26	0.85	2.48	0.11	15.73	0.57	3.05	0.21
36.43	22.34	0.97	2.30	0.09	17.24	0.67	1.70	0.03

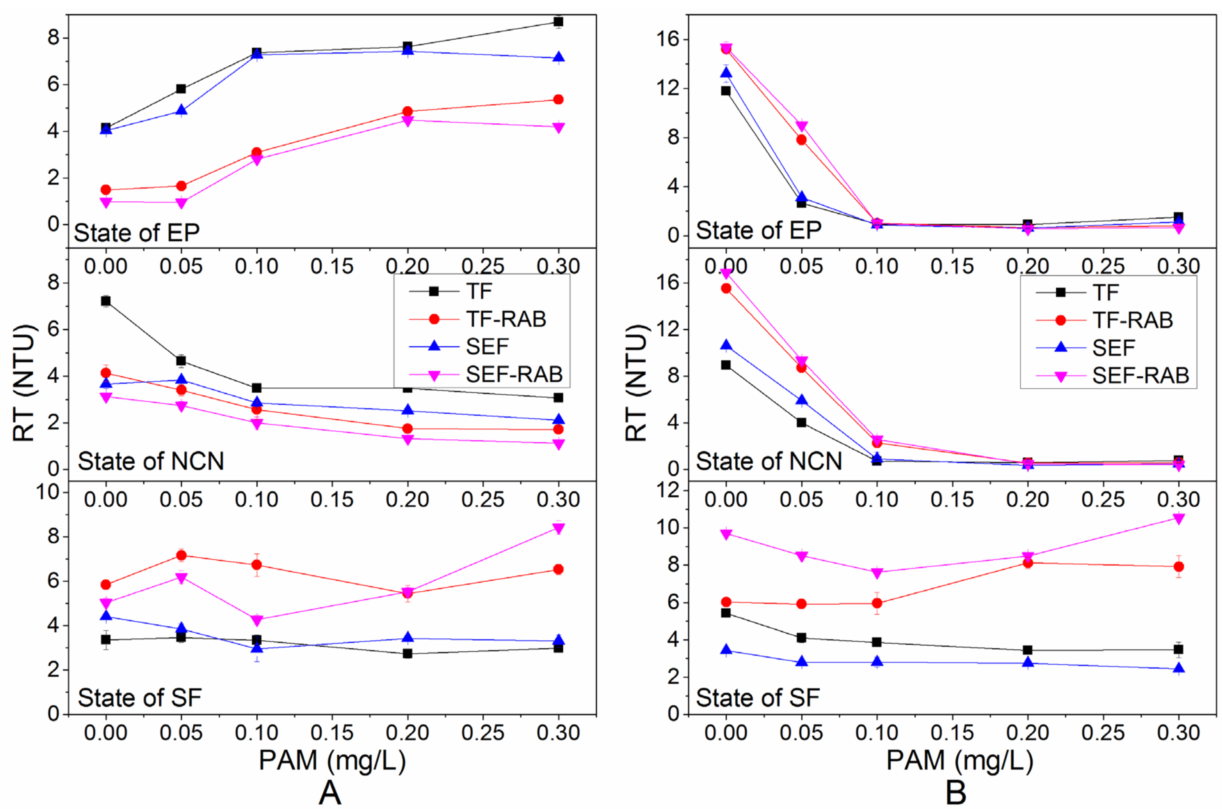

Fig. 2. Residual turbidity at different PAM dosages (Molecular weight of PAM, 18 million Da). A) System I, B) System II.

For System II (Fig. 2b), it was found that under the EP and NCN conditions, the increase in PAM addition obviously enhanced turbidity removal. When the reaction was in the EP state, without adding PAM or with low dosage of PAM under 0.05 mg/L, the SEF did not play a reinforcement role on TF; however, when the dosage increased to 0.10 mg/L, the SEF showed the reinforcement effect. When reaction was in the state of NCN and the PAM dosage was greater than 0.20 mg/L, it was also found that the effect of SEF changed from no reinforcement to strong reinforcement. With the addition of PAM, the residual turbidity changed from an increasing to decreasing trend for the RAB of these two flocculation types. When the reaction was in the state of SF, with any PAM dosage, the residual turbidity of TF-RAB was higher than that of TF, while the residual turbidity of SEF was lower than that of TF. This suggests that in the SF state, the addition of PAM could not change the effect of SEF and TF-RAB on TF.

The above results showed that the increase in PAM dosage can change the effectiveness of SEF in System II. Selection of the appropriate additive dosage can change the effect of the SEF on TF from increase to decrease in residual turbidity.

When both the systems were in the SF charge state, addition of PAM did not change the effectiveness of SEF, which showed that the addition of PAM did not have significant influence in the SF state. Moreover, by comparing the change of TF-RAB compared with that of TF residual turbidity, it could be observed that in the presence of long chain molecule bridging, the relationship between SEF and TF was strongly correlated to the performance of RAB as well.

3.3. Floc growth

The floc growth and its corresponding factors of TF and SEF in System I at different PAM dosages are shown in Fig. 3.

When System I was in the EP state (Fig. 3a) and the PAM dosage was 0 mg/L, the average floc sizes of SEF and TF after stopping the rapid mixing were 126.43 µm and 176.49 µm, respectively. When the PAM dosage was 0.05 mg/L, the average floc sizes increased slightly to 127.14 µm and 196.08 µm, respectively, but when the dosage was 0.10 mg/L, these values were only 118.83 µm and 152.04 µm, respectively. This result indicates that the floc growth of TF and SEF was inhibited to a certain degree, and the addition of PAM had a colloidal protection effect. When the dosage increased to 0.30 mg/L, these values decreased to 89.28 µm and 102.61 µm, respectively. On the other hand, it appears that the inhibition phenomena of floc growth, this study found that the of floc for both TF and SEF decreased gradually with the increase in PAM addition, while the increased gradually. When the dosage was 0.20 mg/L, the floc B_f was close to zero for TF and SEF (0.015 and 0.073, respectively), and the was close to 2 (1.72 and 1.97, respectively); when the dosage was 0.30 mg/L, the enforced breakage did not lead to a drop in average floc size. Instead, the average particle size increased sharply, and the floc Rg_f reached 1.97 µm and 2.72 µm, respectively.

When System I was in the state of NCN (Fig. 3b) and the PAM dosage was 0 mg/L, the average floc sizes of SEF and TF after stopping the rapid mixing were 184.68 µm and 205.80 µm, respectively. When the dosage was 0.10 mg/L, the average particle size of flocs increased to 205.88 µm and 300.86 µm, respectively. At this time in the early stage of the floc growth, the inhibition phenomenon had appeared. When the dosage was 0.20 mg/L, the floc sizes were only 191.33 µm and 286.78 µm, respectively, which meant the colloidal protection effect had appeared. When the dosage was 0.30 mg/L, the sizes were as low as 147.94 µm and 217.58 µm, respectively. Different from state of EP (Fig. 3a), the TF B_f gradually reduced as the PAM dosage increased, while the Rg_f gradually increased. However, the B_f of SEF first increased and then decreased, while the Rg_f increased after falling first. When the dosage was 0.05 mg/L both factors reached their peak values. When the dosage was 0.20 mg/L, both their Rg_f were greater than 1 (1.65 and 1.25, respectively), indicating the complete reversibility after floc breakage.

When System I was in the state of SF (Fig. 3c), the increase in PAM dosage did not have much impact on the floc size. The floc size remained between 141.73 µm and 153.16 µm after stopping TF agitation, and for SEF, the size remained between 153.28 µm and 161.33 µm. Both their B_f and Rg_f were stable. The B_f of SEF was maintained between 0.47 ~ 0.49, which was lower than that of the TF (0.57 ~ 0.64), and the Rg_f of SEF was maintained between 0.73 ~ 0.75, which was higher than that of the TF (0.61 ~ 0.6).

The floc growth and its corresponding factors of TF and SEF in System II at different PAM dosages are shown in Fig. 4.

When System II was in the EP (Fig. 4a) and NCN (Fig. 4b) states and the PAM dosage was 0.20 mg/L, it was observed that the TF floc growth was restrained. After stopping the agitation, the floc size decreased from 302.46 µm and 283.97 µm to 136.43 µm and 227.08 µm, respectively, when the dosage was 0.10 mg/L. Although the SEF floc growth in early stage was severely suppressed, the later rapid growth after stopping stirring resulted in the floc size (321.00 µm and 405.43 µm) still being higher than that of TF when the dosage was 0.20 mg/L. Until the dosage was 0.30 mg/L, the SEF flocs growth was severely inhibited.

In these two kinds of states, the changes in break age properties of flocs were different compared to System I. The B_f of TF and SEF both increased first, and then decreased. In the EP state, when the PAM dosage was 0.10 mg/L, the B_f of TF and SEF reached the peak values, which were 0.68 and 0.63, respectively. When the PAM dosage was 0.20 mg/L, the B_f showed a sharp decrease, indicating that the TF crushing operation did not lead to a drop in the average particle size. The SEF B_f dropped to 0.51, and the Rg_f of both TF and SEF were greater than 1 (2.68 and 1.52, respectively). In the NCN state, the breakage property of TF reached the maximum value when the dosage was 0.10 mg/L (0.70). For SEF, the breakage property reached the maximum at the dosage of 0.20 mg/L (0.66), and then showed a sharp decline, which was the same as in EP state. When the dosage was 0.20 mg/L, the Rg_f of both were greater than 1 (1.41 and 1.02, respectively).

System II in the SF state (Fig. 4c) was similar to System I. Moreover, the addition of PAM and its dosage did not have much impact on the flocs' growth, breakage, and the recovery performance. The floc size of TF after stopping the stirring remained between 128.41 µm and 151.74 µm, and for SEF, the floc size remained between 132.19 µm and 150.11 µm. The B_f of TF was between 0.54 and 0.64, which was higher than that of the SEF (0.47 ~ 0.49). Also, the Rg_f of TF was between 0.58 and 0.66, which was lower than that of the SEF (0.70 ~ 0.75).

Comparing the Rg_f and B_f of flocs formed by the SEF and TF, it was found that in the presence of long chain molecule bridging, the flocs recoveryability for SEF and TF in different charge states was in the following order: EP > NCN > SF. However, under the same charge state conditions, there were considerable differences in the breakability and recovery ability of flocs formed by SEF compared to TF.

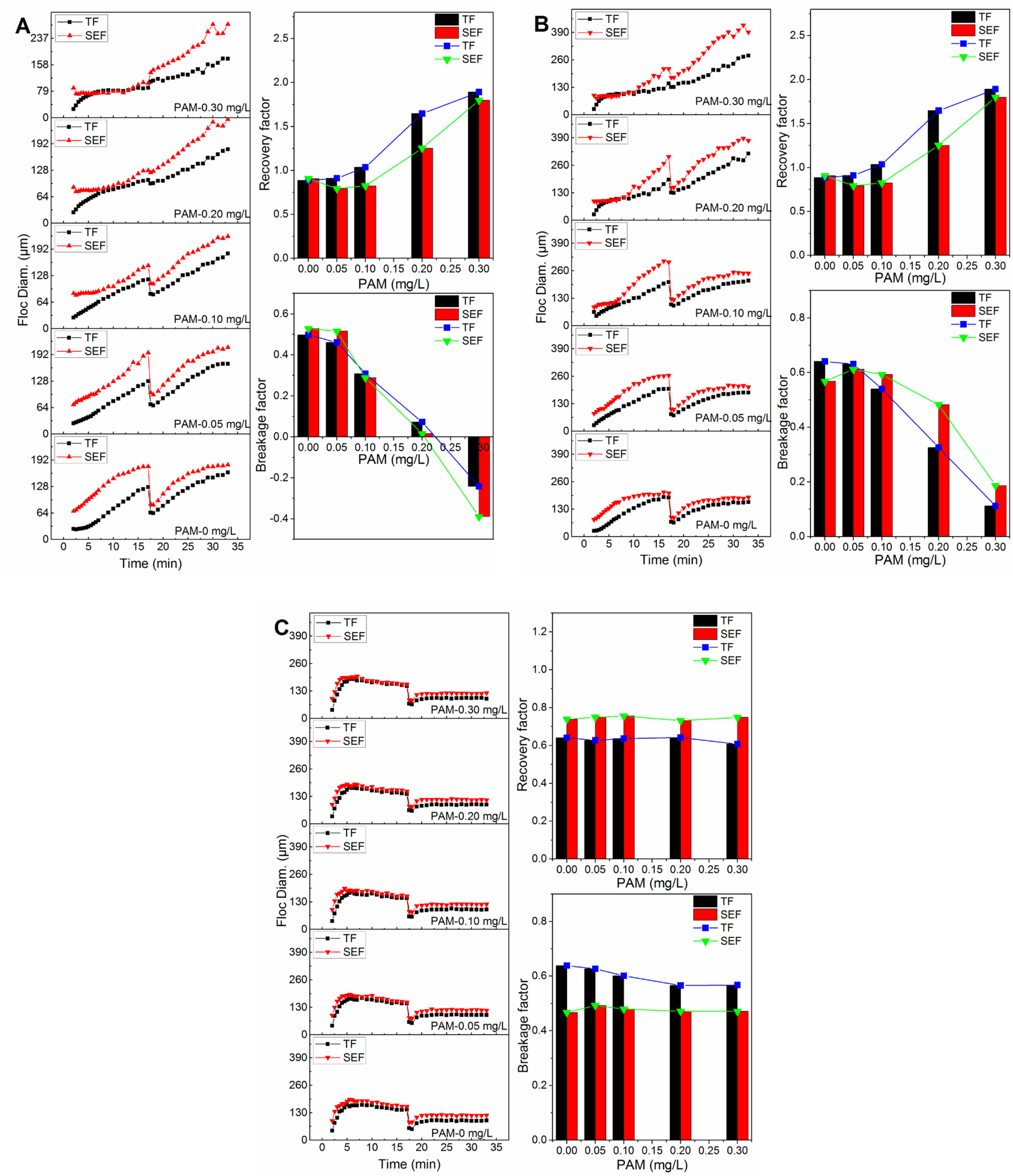

Fig. 3. Floc growth and its factors in System I at different PAM dosages. A) State of EP, B) State of NCN, C) State of SF.

For System I in the EP state, when the PAM dosage was 0.10 mg/L, the flocs breakability of SEF was lower than that of TF. When the PAM dosage reached 0.20 mg/L, the recovery ability of SEF was much higher than that of TF. In the NCN state, when the PAM dosage was 0.10 mg/L, the flocs breakability of SEF was higher than that of TF. Moreover, as long as there was PAM addition, the Rg_f of SEF was lower than that of TF.

For System II, from the point of breakability, under EP and NCN states, the change of B_f of the floc with TF and SEF

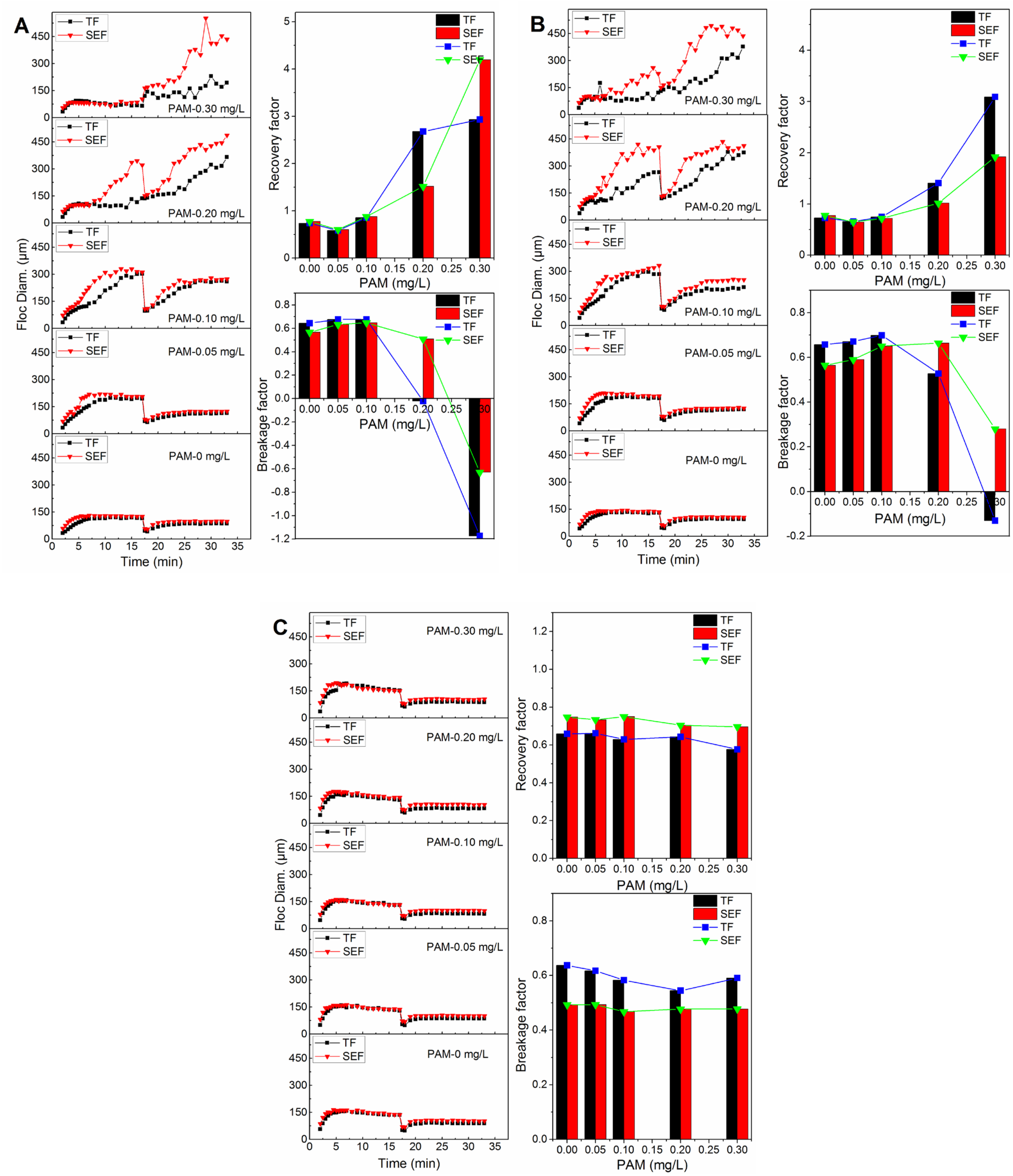

Fig. 4. Floc growth and its factors in System II at different PAM dosages. A) State of EP, B) State of NCN, C) State of SF.

flocculation ways with PAM dosage variation was similar to that in the NCN state of System I. When the PAM dosage was relatively low, the B_f of SEF floc was lower than that of TF. It can be attributed to the fact that the average floc size d_b after an enforced break operation of SEF was significantly greater than that of TF. This is because of, on the one hand, the adsorption of the PAM chain to the raw colloid, small broken flocs or new small flocs; on the other hand, the adsorption of small broken flocs to the raw colloid. Conversely, when the dosage was relatively high, the B_f of

SEF floc was higher than that of TF. This is because with relatively high PAM dosage, although the broken floc size increased d_b as well, but the increase is limited. At the same time, the relative increase in the amount of floc size d_c of SEF to TF was much higher than that at lower PAM dosage. Take the dosage of 0.20 mg/L as an example, the d_a for System I in the state of NCN rose from 191.33 μm to 300.78 μm, with the amount of increase reached 57.2%. The amount of increase for System II in EP and NCN states reached 135.3% and 57.4%, respectively. At the dosage of 0.05 mg/L, these increased amounts were only 31.4%, 5.5%, and 7.4%, respectively. In contrast with the EP state of system I mentioned above, this phenomenon is related to the aggregation ways of flocs. In the EP state for TF, at low PAM dosage, no serious colloid protection phenomenon occurred. Although there was adsorption bridging effect, the floc monomer agglomeration still played a dominate role. After adding sludge, a large amount of small broken flocs made the flocculation change into cluster-cluster agglomeration, which led to the increase in breakability. When PAM dosage was high, as analyzed above, the PAM had a strong colloid protection effect and the floc generated by TF was small. There were still considerable unused active positions on the PAM molecular chain that were mainly dominated by the monomer agglomeration on the surface. When the deposited flocs were added, the particle concentration in the system increased, which made full use of the active positions on the PAM chain. As a result, a large number of flocs were formed by monomer agglomeration with bridging molecular chains as the floc skeleton. Even the enforced breakage can hardly strip the monomer agglomerates from the polymer molecular chain, and surface corrosion phenomenon was not observed. The short crushing operation merely caused breakage of the molecular chain, and the majority of monomer agglomerates could not be released, even though the active positions of molecular chain were fully used, thus there was a decrease of breakability. In other words, when the System I was in EP state and the PAM dosage was high, the decrease in SEF flocs breakability was because the effect of the long chain bridging has higher ability to resist the breakage.

For System II in the state of EP, the recovery ability of SEF flocs was better than that of TF. In the NCN state of System II, similar to System I, once PAM was added, the Rg_f of SEF flocs was lower than that of TF. The experiments also showed that in the EP and NCN states, when the PAM dosage was 0.20 mg/L, the Rg_f of flocs formed in the two systems were both greater than 1. This parameter can be used as an indicator to evaluate whether the enhancement of SEF is valid or not.

3.4. Floc morphology

The floc fractal dimensions of TF and SEF at different PAM dosages are shown in Fig. 5.

It can be seen from Fig. 5 that with the increase in PAM dosage, fractal dimension of flocs as a whole was decreased. For System I, in the state of EP, the fractal dimension of SEF flocs was lower than that of TF over the entire dosage. In the NCN state, without addition of PAM, the fractal dimension

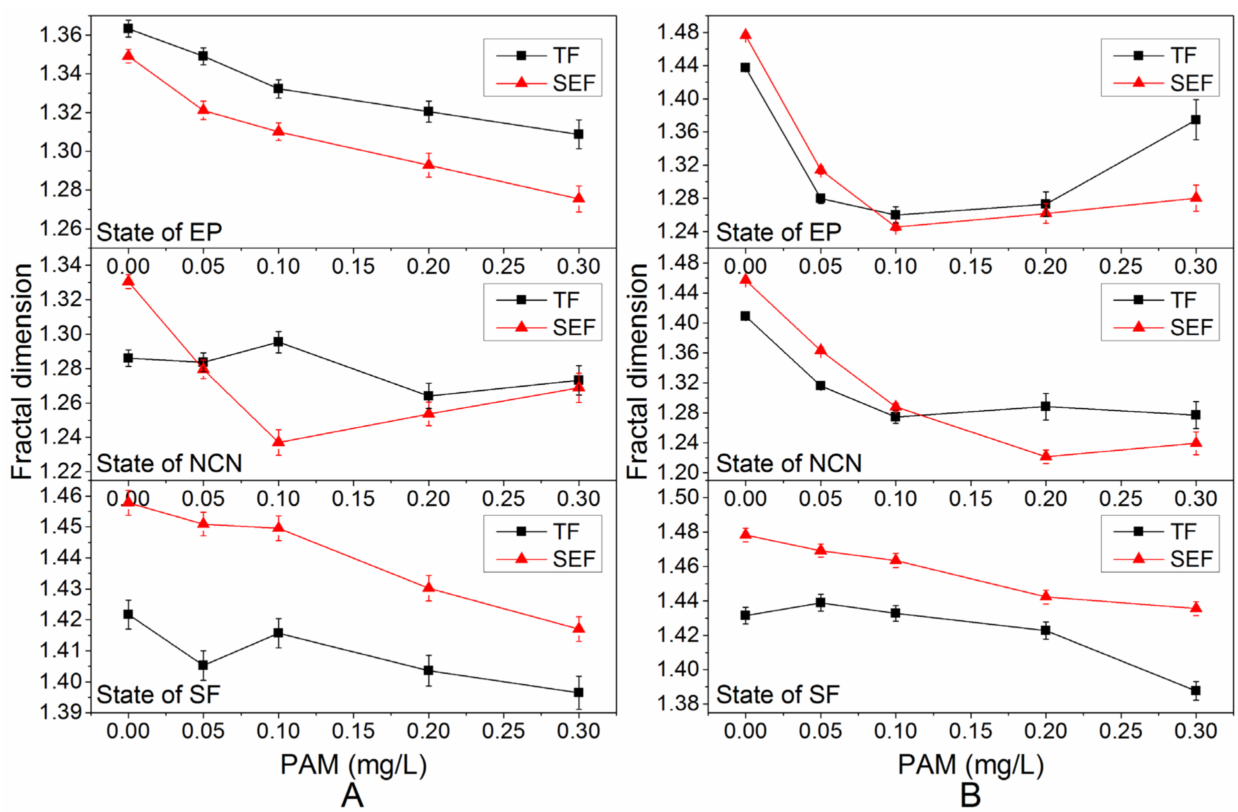

Fig. 5. Floc fractal dimensions of TF and SEF at different PAM dosages. A) System I, B) System II.

of SEF flocs was higher than that of TF; but with the addition of PAM, the situation was reversed. In the state of SF, the flocs fractal dimension of SEF was higher than that of TF over the entire dosage.

For System II, in the EP and NCN states, when the PAM dosage reached a certain concentration, the floc morphology of SEF was better than that of TF. In the EP state, the required PAM dosage was 0.10 mg/L, while in the state of NCN, the required PAM dosage was 0.20 mg/L. In the SF state, the flocs fractal dimension of SEF was always higher than that of TF, which is similar to the results of System I.

The above results showed that in the colloid coagulation mode with charge neutralization, addition of a certain amount of PAM improved the floc morphology of SEF, which was superior to that of TF.

3.5. Floc size distribution

The floc size distributions in Systems I and II in EP and NCN states for the SEF and TF after stopping the agitation are shown in Figs. 6 and 7.

At the different dosages of PAM, the floc frequency distribution and the fitting of Gaussian distribution curve changed greatly. The peak height of Gaussian distribution curve represents the frequency of peak particle size, and the peak width represents the range of particle size distribution. In general, the greater the peak width, the more extensive the size distribution.

As shown in Fig. 6, for System I, the increase in PAM dosage reduced the floc total frequency. Without PAM addition, in the EP and NCN states, the floc total frequencies of SEF were 2875 and 2146, respectively. When the dosage was low, in the state of EP, the total frequencies of SEF floc were 1642 and 1219, respectively. When the dosage was high, in the state of EP, the total frequencies of SEF floc were 1095 and 433, respectively. However, it can be seen from Fig. 6 that SEF caused an increase in the frequencies of all the large flocs.

In the state of EP (Fig. 6a), the size distribution of floc was still mainly small flocs (<50 μm). When the PAM dosage was low (0.05 mg/L), the small flocs frequency decreased the most, and when the PAM dosage was higher (0.20 mg/L), the decrease in small flocs frequency was the lowest. In the state of NCN (Fig. 6b), the small flocs frequency was much less than that in EP state. Without PAM (0.00 mg/L), the small flocs frequency of the SEF floc was 171, which was slightly higher than the 142 of TF. With the addition of PAM (0.05 mg/L and 0.20 mg/L), the small flocs frequencies of SEF floc were 90 and 130, respectively, compared to the frequencies of 124 and 173 for TF at the same PAM dosage. Considering the fitted Gaussian distribution curve at different dosages, the peak of SEF flocs distribution moved towards the larger size, indicating that the large size floc frequency increased. Among the different dosages, when the PAM dosage was lower (0.05 mg/L), the flocs distribution range was narrower, and when the dosage was higher (0.20 mg/L), the flocs had a wider distribution range.

It can be seen from Fig. 7 that for System II, the total floc frequency decreased with the increase in PAM dosage. In the EP and NCN charge states, without addition of PAM, the total frequencies of SEF flocculent were 5897 and 5074,

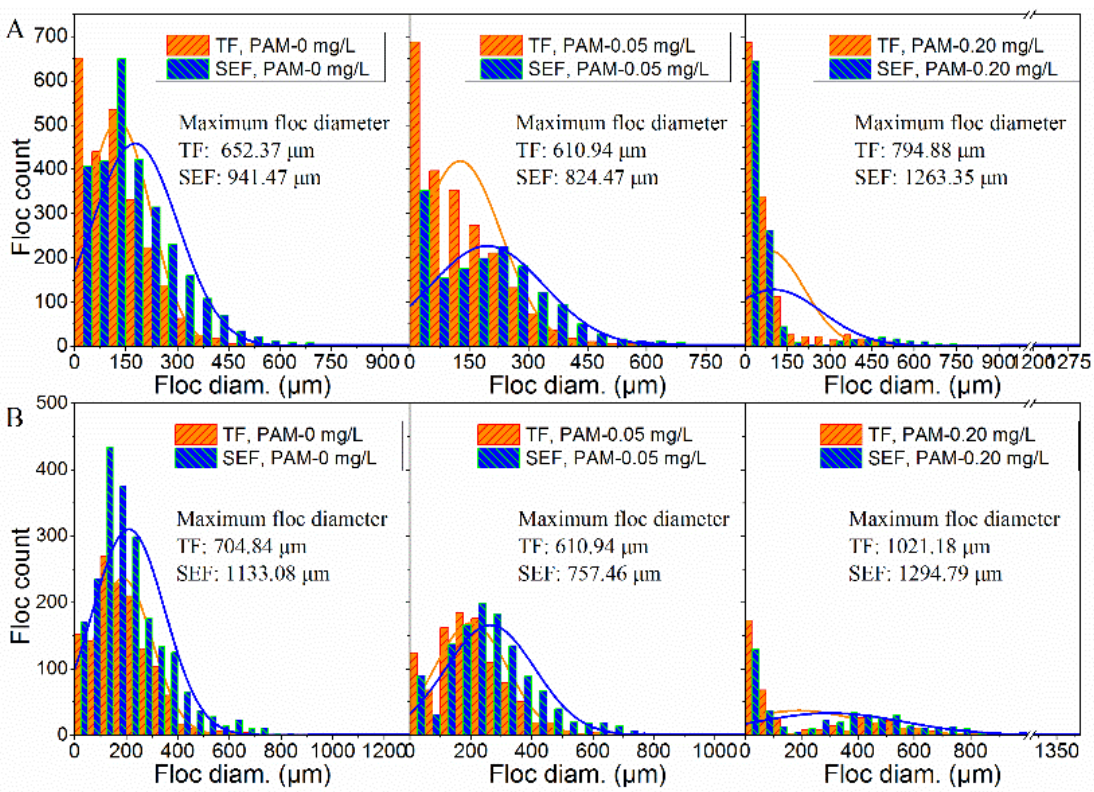

Fig. 6. Floc size distributions of TF and SEF at different PAM dosages (System I). A) State of EP, B) State of near NCN.

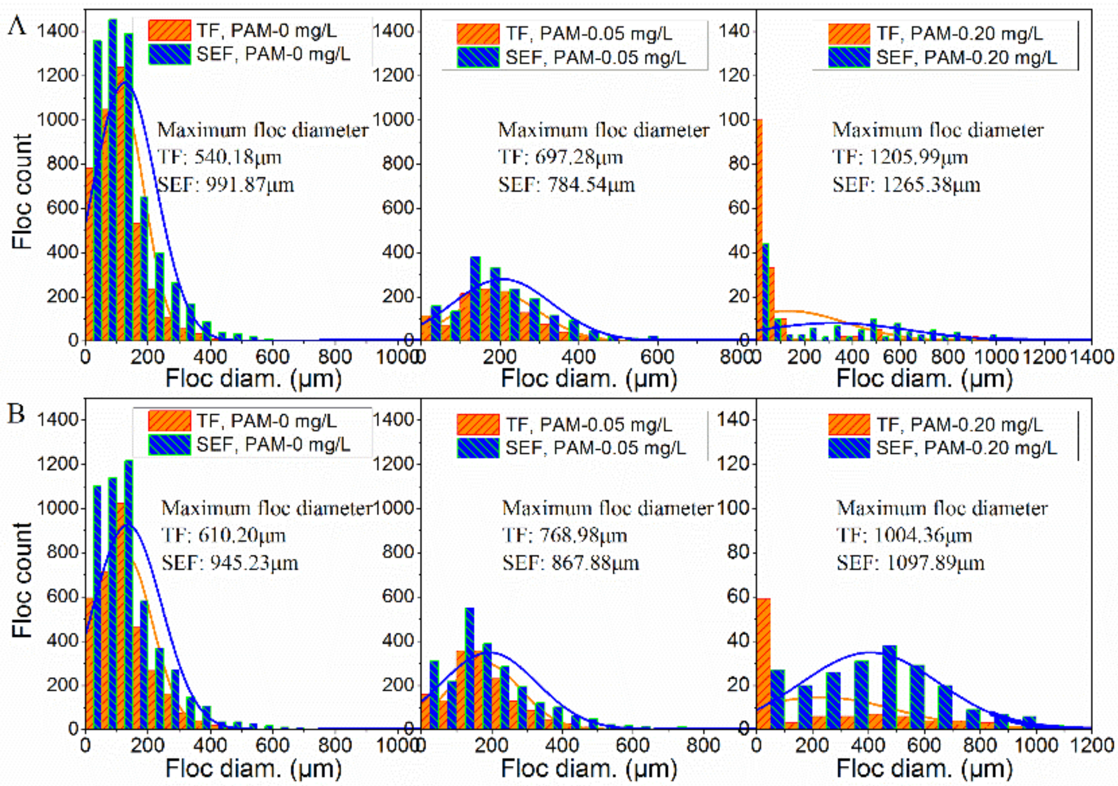

Fig. 7. Floc size distributions of TF and SEF at different PAM dosages (System II). A) State of EP, B) State of NCN.

respectively. When the added PAM dosage was low (0.05 mg/L), the total frequencies of SEF flocculent were 1776 and 2365, respectively. When PAM dosage was higher, the total frequencies of SEF flocculent decreased to 128 and 215, respectively.

From the perspective of small flocs frequency, in the EP and NCN charge states without the addition of PAM (0.00 mg/L), the small flocs frequencies of SEF were 1358 and 1130, respectively, which were substantially higher than those of TF (783 and 595, respectively). The peak of the Gaussian distribution curve did not show any substantial change. When the PAM dosage was low (0.05 mg/L), although the small flocs frequency was low, the small flocs frequency of SEF still increased relatively faster than that of TF. Also, the peak of Gaussian distribution curve was slightly offset. When PAM was higher (0.20 mg/L), the small flocs frequencies of SEF were 44 and 19, respectively, which were substantially lower than those of TF (100 and 48). Considering the flocs distribution range, the flocs distribution range of TF increased with the increase in PAM dosage. However, for the SEF, low dosage of PAM led to smaller flocs distribution range, while high dosage of PAM made the flocs distribution wider, similar to the results of System I.

4. Conclusions

The main conclusions of this work are as follows:

(1) In the kaolin colloid system, the increase in PAM dosage didnot change the effect of SEF on TF. In the humic acid - kaolin colloid system, without addition of PAM, the reinforcement effect of SEF on TF could not be observed. However, when the dosage reached 0.10 mg/L in the EP state and reached 0.20 mg/L in the NCN state, the PAM dosage was able to bring about the SEF reinforcement effect on TF.

(2) Without PAM addition, the SEF flocs recovery ability was stronger than that of TF. The PAM addition can improve the flocs, and reduce. On the other hand, with the increase in PAM dosage, the SEF recovery ability was weaker than that of TF, but its breakability was higher than that of TF, in most cases.

(3) In the colloid coagulation mode which gives priority to charge neutralization, adding a certain amount of PAM improved the SEF floc morphology, which was better than that of TF. As a result, the process of settlement was enhanced, leading to better effluent quality.

(4) The increase in PAM dosage reduced the small flocs frequency, which could be attributed to the immediate enhancement effect of SEF. Compared to absence of PAM, the low PAM dosage narrows the flocs distribution range, while a high PAM dosage makes flocs distribution range wider.

(5) When the sweep flocculation dominated the coagulation mechanism, the increase in PAM dosage had little impact on the SEF and TF flocs growth, breakage, and recovery performance. Although the PAM

dosage could improve the floc morphology, the SEF floc morphology remained worse than that of the TF. The increase in PAM dosage did not enable the enhancement effect of SEF. Therefore, the increase in PAM dosage is not relevant in the charge state of sweep flocculation.

Aknowledgements

This research was supported by the National Natural Science Foundation of China (Number:51478274) and Foundation for Distinguished Young Talents in Higher Education of Guangdong, China (Number:2014kqncx105).

References

[1] N.A. Oladoja, Advances in the quest for substitute for synthetic organic polyelectrolytes as coagulant aid in water and wastewater treatment operations, Sustain. Chem. Pharm., 3 (2016) 47–58.

[2] D. Li, X. Li, H. Zhang, F. Li, S. Qian, S.W. Joo, Efficient heat transfer enhancement by elastic turbulence with polymer solution in a curved microchannel, Microfluid. Nanofluid., 21 (2017) 10.

[3] G. Sen, S. Mishra, K. Prasad Dey, S. Bharti, Synthesis, characterization and application of novel polyacrylamide-grafted barley, J. Appl. Polym. Sci., 131 (2014).

[4] D. Zhao, H. Liu, W. Guo, L. Qu, C. Li, Effect of inorganic cations on the rheological properties of polyacrylamide/xanthan gum solution, J. Nat. Gas. Sci. Eng., 31 (2016) 283–292.

[5] V.H. Dao, N.R. Cameron, K. Saito, Synthesis, properties and performance of organic polymers employed in flocculation applications, Polym. Chem-UK, 7 (2016) 11–25.

[6] J. Wang, S. Yuan, Y. Wang, H. Yu, Synthesis, characterization and application of a novel starch-based flocculant with high flocculation and dewatering properties, Water Res., 47 (2013) 2643–2648.

[7] W. Rudolfs, H.W. Gehm, Chemical coagulation of sewage. VI. Clarifying value of return sludge, Sewage Works J., 9 (1937) 22–33.

[8] R.A. Stevenson, P.J. Beard, H.O. Banks, Chemical sewage purification at Palo Alto. Regeneration of spent coagulant effects complete sewage treatment, Sewage Works J., 5 (1933) 53–60.

[9] L.H. Enslow, Chemical precipiation processes, Civil Eng., 5 (1933) 234–239.

[10] K. Loganathan, P. Chelme-Ayala, M. Gamal El-Din, Effects of different pretreatments on the performance of ceramic ultrafiltration membrane during the treatment of oil sands tailings pond recycle water: A pilot-scale study, J. Environ. Manage., 151 (2015) 540–549.

[11] L.L. Miao, M.W. Zhu, J.X. Duan, Q.L. Zhu, H.Y. Sun, Efficient sedimentation/MBBR/filter for treatment of metallurgical comprehensive wastewater, China Water Wastewater, 28 (2012) 47–50.

[12] D.G. Stevenson, A review of current and developing potable water treatment processes, Proc. Inst. Mech. Eng., Part E: J. Process Mech. Eng., 217 (2003) 11–23.

[13] W. Wei, X. Li, J. Zhu, M. Du, Characteristics of flocs formed by polyaluminum chloride during flocculation after floc recycling and breakage, Desal. Water Treat., 56 (2015) 1110–1120.

[14] L. Sun, M. Lv, Y. Yang, J. Lin, L. Zhou, G. Li, Enhanced treatment of water with low turbidity: Combined effects of permanganate, PAM and recycled sludge, J. Harbin Inst. Technol. (New Ser.), 6 (2009) 25.

[15] S. Liu, T. Liang, Return sludge employed in enhancement of color removal in the integrally industrial wastewater treatment plant, Water Res., 38 (2004) 103–110.

[16] B. Wang, Z. Chen, J. Zhu, J. Shen, Y. Han, Pilot-scale fluoride-containing wastewater treatment by the ballasted flocculation process, Water Sci. Technol., 68 (2013) 134–143.

[17] Z. Zhou, Y. Yang, X. Li, W. Gao, Coagulation performance and flocs characteristics of variable sludge recycling designs for the synthetic low–turbidity water treatment, Desal. Water Treat., 52 (2014) 4705–4714.

[18] Z. Zhou, Y. Yang, X. Li, W. Gao, H. Liang, G. Li, Coagulation efficiency and flocs characteristics of recycling sludge during treatment of low temperature and micro-polluted water, J. Environ. Sci. (China), 24 (2012) 1014–1020.

[19] S.J. Jiang, X.Y. Long, Y. Zhang, P.F. Wang, Pilot study of yangtze river water treatment in the winter by sludge return, Appl. Mech. Mater., 209–211 (2012) 1915–1922.

[20] Y. Xu, B. Cui, R. Ran, Y. Liu, H. Chen, G. Kai, J. Shi, Risk assessment, formation, and mitigation of dietary acrylamide: Current status and future prospects, Food Chem. Toxicol., 69 (2014) 1–12.

[21] A. Guezennec, C. Michel, K. Bru, S. Touzé, N. Desroche, I. Mnif, M. Motelica-Heino, Transfer and degradation of polyacrylamide-based flocculants in hydrosystems: a review, Environ. Sci. Pollut. R., 22 (2015) 6390–6406.

[22] P. Erkekoglu, T. Baydar, Acrylamide neurotoxicity, Nutr Neurosci, 17 (2014) 49–57.

[23] Z. Wang, J. Nan, M. Yao, Y. Yang, X. Zhang, Insight into the combined coagulation-ultrafiltration process: The role of Al species of polyaluminum chlorides, J. Membr. Sci., 529 (2017) 80–86.

[24] M.A. Yukselen, J. Gregory, The reversibility of floc breakage, Int J. Miner. Process., 73 (2004) 251–259.

[25] P. Jarvis, B. Jefferson, J. Gregory, S.A. Parsons, A review of floc strength and breakage, Water Res., 39 (2005) 3121–3137.

[26] J. Sun, L. Qin, G. Li, Y. Kang, Effect of hydraulic conditions on flocculation performances and floc characteristics in Chinese herbal extracts by chitosan and chitosan hydrochloride, Chem. Eng. J., 225 (2013) 641–649.

[27] P. Bubakova, M. Pivokonsky, P. Filip, Effect of shear rate on aggregate size and structure in the process of aggregation and at steady state, Powder Technol., 235 (2013) 540–549.

[28] W. He, J. Nan, H. Li, S. Li, Characteristic analysis on temporal evolution of floc size and structure in low-shear flow, Water Res., 46 (2012) 509–520.

[29] M. Soos, A.S. Moussa, L. Ehrl, J. Sefcik, H. Wu, M. Morbidelli, Effect of shear rate on aggregate size and morphology investigated under turbulent conditions in stirred tank, J. Colloid. Interf. Sci., 319 (2008) 577–589.

[30] C. Ye, D. Wang, B. Shi, J. Yu, J. Qu, M. Edwards, H. Tang, Alkalinity effect of coagulation with polyaluminum chlorides: Role of electrostatic patch, Colloids Surf. A: Physicochem. Eng. Asp., 294 (2007) 163–173.

[31] X. Wu, X. Ge, D. Wang, H. Tang, Distinct coagulation mechanism and model between alum and high Al 13-PACl, Colloids Surf. A: Physicochem. Eng. Asp., 305 (2007) 89–96.